Microcellular Foaming of Poly(lactic acid)/Silica Nanocomposites in Compressed CO2: Critical Influence of Crystallite Size on Cell Morphology and Foam Expansion

ARTICLE *in* INDUSTRIAL & ENGINEERING CHEMISTRY RESEARCH · MAY 2013

Impact Factor: 2.59 · DOI: 10.1021/ie302281c

6 AUTHORS, INCLUDING:

Wentao Zhai
Chinese Academy of Sciences
62 PUBLICATIONS **978** CITATIONS
SEE PROFILE

Wen-Ge Zheng
Chinese Academy of Sciences
50 PUBLICATIONS **1,218** CITATIONS
SEE PROFILE

I&EC research
Industrial & Engineering Chemistry Research

Article

pubs.acs.org/IECR

Microcellular Foaming of Poly(lactic acid)/Silica Nanocomposites in Compressed CO_2: Critical Influence of Crystallite Size on Cell Morphology and Foam Expansion

Guoying Ji,[†] Wentao Zhai,*[,†] Dongpo Lin,[†] Qian Ren,[‡] Wenge Zheng,[†] and Dong Won Jung*[,§]

[†]Ningbo Key Lab of Polymer Materials, Ningbo Institute of Material Technology and Engineering, Chinese Academy of Sciences, Ningbo, Zhejiang Province, 315201, China

[‡]Hunan Normal University, College Chemistry & Chemical Engineering, Changsha 410081, Hunan, China

[§]Department of Mechanical Engineering, Cheju National University, 690-756 Jeju-do, Republic of Korea

ABSTRACT: During the solid state foaming, the CO_2 saturated poly(lactic acid) (PLA) sample at 5 MPa and 20 °C has a high crystallinity of 23.2%, and the prepared PLA foams exhibits low foam expansion and nonuniform cell structure. This study presents an interesting effect of nanosilica addition on the cell morphology and expansion ratio of PLA foams. It was found that the presence of nanosilica increased the induced crystallinity of PLA up to 29.7% at 5 MPa. The resultant PLA/silica foams exhibited significant and concurrent increase in cell structure uniformity and cell density: the cell density increased about 5−10 times, the expansion ratio increased 1.4−2.1 times, and the crystallinity of foams increased 1.3 times, compared to pure PLA foams. Further investigation suggested that the formation of the tiny crystallite size and the well dispersed nanosilica aggregates were thought as the main reasons to explain the interesting effect of nanosilica addition on the foaming behavior of PLA.

INTRODUCTION

Biomass-derived poly(lactic acid) (PLA) is one of the most promising materials because it is biodegradable and biocompatible. The applications of PLA in the biomedical, tissue engineering, and packaging fields, therefore, have been explored extensively in the past decades.[1−4] Unfortunately, PLA has a low service temperature, due to its low glass transition temperature and low crystallization kinetics, which significantly limits its uses in many applications. To provide PLA based products with a high service temperature, high crystallinity is critical.

Microcellular foaming technology has been verified to increase the crystallinity of PLA,[5−12] because of the strong plasticization effect of blowing agent during the saturation process and the applied strong extensional flow during the foam expansion process. Marubauashi et al. found that the crystallinity of poly(L-lactide) (PLLA) saturated at 7−15 MPa and 0−80 °C could reach 45%.[5] Our previous study indicated that the equilibrium crystallinity of PLA saturated at 6.89 MPa and 100 °C was about 38.3%, and a short saturation time of 25 min was long enough to reach the maximum crystallinity value.[6] At a low CO_2 pressure of 5 MPa, the saturated PLA presented low crystallinity of about 23.0%.[7,9] The effect of foam expansion process on the crystallinity of PLA has been investigated by researchers.[6−8] It was reported that the crystallinity of the saturated PLA at 5 MPa was 23.4%, while the crystallinity of foamed PLA at 60 °C was 29.7%.[7] An increase in foaming temperature tended to increase the crystallinity of PLA foam slightly up to 31.4% at 80 °C.[7] A quantificational investigation of the effect of stretching on PLA's crystallization has been carried out by Mihai et al. using a Brückner Biaxial Lab Stretcher at a constant stretch speed of 1 m/min.[8] They found that biaxial stretching could induce significant crystallinity in a time frame similar to that expected for foam expansion and cooling.

The presence of crystallites tends to significantly affect the polymeric foaming process and thereby determines the cell morphology, expansion ratio, and crystallinity of the resultant foams.[6,7,13−18] In general, the crystallite-induced heterogeneous cell nucleation increases the cell density and decreases the cell size.[14,15] Once the induced crystallinity is too high or the formed crystalline domains are too large, the crystallite tends to impose considerable hindrance to the formation of uniform and evenly distributed cells.[17] A systemic study of the evolution of cell structure with the crystallinity of saturated PLA had been investigated,[6] where a pressure quenching procedure was applied and the resin's crystallinity was adjusted by the saturation time. At 6.89 MPa/100 °C for 1 min, PLA foam with very few large bubbles was observed across the thickness direction. With a slight extension of saturation time from 1 to 3, to 5, and to 10 min, a significant increase in cell density, which was accompanied by a gradual increase in foam expansion, was seen. At 10 min, the cell structure distribution tended to be uniform, and the obtained crystallinity and expansion ratio of PLA foam was 30.2% and 15.8, respectively. A further increase in saturation time increased the cell density and induced the formation of a nonuniform cell structure distribution. At 120 min, the PLA sample could not foam, because too high of a crystallinity (38.8%) had been achieved before foaming. These results suggests that it is very challenging to fabricate a semicrystalline polymeric foam with a high expansion ratio and

Received: August 26, 2012
Revised: April 18, 2013
Accepted: April 22, 2013
Published: April 22, 2013

dx.doi.org/10.1021/ie302281c | *Ind. Eng. Chem. Res.* 2013, 52, 6390−6398

the well-defined cell structure once the gas-saturated sample has a high crystallinity.

Our previous study demonstrated that the presence of ultrasonic irradiation was helpful for the preparation of PLA foam with a high cell density of 10^9 cells/cm^3, high expansion ratio of 10−14, and high crystallinity of 31%, even though the saturated PLA possessed a high induced crystallinity of 23.4%, which was attributed to the enhanced cell nucleation of ultrasonic irradiation.[7] It is well accepted that the nanoparticle is a kind of crystallization nucleating agent, and it tends to decrease the crystal size and increase the crystal density of the semicrystalline polymer. Furthermore, the nanoparticles and the formed crystalline domains can induce the heterogeneous cell nucleation during foaming.[13,16,18,19] It is interesting to figure out whether the nanoparticles fabricate both the crystallinity development and the improvement of cell structure.

In this study, microcellular foaming technology using CO_2 was carried out to foam PLA, and the nanosilica was selected as a nucleating agent. The target of this investigation is to fabricate PLA foams with high crystallinity, uniform cell morphology, and high expansion ratio. The critical influence of crystallite size on the cell morphology and expansion ratio of PLA foams was emphasized.

EXPERIMENTAL SECTION

Materials and Sample Preparation. A semicrystalline PLA (Ingeo, 2002D) in pellet form was obtained from NatureWorks LLC. According to the supplier, its D-isomer content is 4.3%, and its density is 1.24 g/cm^3. Silica, AEROSIL200, manufactured by Evonik, is a hydrophilic fumed silica with a specific surface area of 200 m^2/g and an average primary particle size of 12 nm. CO_2 with a purity of 99.9% obtained from Ningbo Wanli Gas Corporation was used as the physical blowing agent. The PLA and silica were vacuum-dried at 80 °C for 8 h before use. The PLA/silica nanocomposites were melt extruded using a counter-rotating twin-screw mini compounder by maintaining a temperature of 200 °C with a screw speed of 200 rpm. The silica content prepared for the master batch was 7 wt %. A series of nanocomposites with a silica content of 0.5, 1, 3, 5, and 7 wt % was obtained by diluting the masterbatch with the PLA and were thereafter coded as PLAS0.5, PLAS1.0, PLAS3.0, PLAS5.0, and PLAS7.0, respectively. Pure PLA was also processed in the same condition for a comparison purpose. Specimens with thickness of 0.8 mm were prepared by compression molding at 185 °C and then quenched to room temperature by cold water. The crystallinities of the as-prepared PLA and PLAS nanocomposites were 0%. The sheets were cut into specimens with dimensions of 20 mm × 20 mm for foaming experiments.

Batch Foaming. The PLAS nanocomposites sheets were placed in a high-pressure vessel at 20 °C. The vessel was flushed with low-pressure CO_2 for about 1 min and then pressurized to 5 MPa. The samples were saturated under this condition for 12 h to ensure equilibrium adsorption of CO_2. At the end of the experiment, the specimens were removed from the vessel after a rapid quench of pressure and were transferred within 1 min to the water bath with the fixed temperature. The foamed samples were quenched in cold water with the temperature of 15 °C after 20 s of foaming.

Characterization. The crystallinity of PLAS nanocomposites was determined using an apparatus (Mettler Toledo differential scanning calorimetry/thermogravimetric analysis (DSC/TGA)) calibrated with indium. For all samples, only data obtained from the first heating for assessing the possible effect of the CO_2 saturation and the foaming process on the crystallization behavior of the PLA. For all CO_2 saturated samples, a long time degassing (more than 1 month) was carried out to remove the possible effect of gas plasticization on the sample's crystallinity. The heating rate of the DSC tests was fixed at 10 °C/min. The degree of crystallinity was calculated by $[(\Delta H_m - \Delta H_c)/\Delta H_f] \times 100\%$, where ΔH_c is the heat of fusion generated by the cold crystallization and ΔH_f is the theoretical heat of fusion of 100% crystalline PLA with a value of 93 J/g.[20]

The mass densities of the samples before (ρ) and after (ρ_f) foaming were measured by the water displacement method based on ISO 1183-1987. The uptake of water by the samples during this measurement can be neglected due to the samples' smooth skin and closed cells.

The dispersion of nanosilica in the PLA matrix and the morphology of the foamed samples were observed with a Hitachi TM-1000 scanning electron microscope (SEM). The samples were freeze-fractured in liquid nitrogen and sputter-coated with gold. Cell size and cell density were determined from SEM micrographs. The cell diameter was on average at least a size of 100 cells on the SEM micrographs. The cell density (N_0), the number of cells per cubic centimeter of solid polymer, was determined using eq 1 as follows:

$$N_0 = \left[\frac{nM^2}{A}\right]^{3/2} \phi \tag{1}$$

where n is the number of cells in the SEM micrograph, M is the magnification factor, A is the area of the micrograph (in cm^2), and ϕ is the volume expansion ratio of the polymer foam, which can be calculated using eq 2 as follows:

$$\phi = \frac{\rho}{\rho_f} \tag{2}$$

where ρ and ρ_f are the densities of PLA resin and PLA foam.

The dispersion of nanosilica in PLA matrix was further studies by TEM (Tecnai G2 F20) with an accelerating voltage of 200 keV. Prior TEM observation, ultrathin sections about 100 nm in thickness were directly cut with a diamond knife.

The dynamic mechanical analysis (DMA) of neat PLA and PLAS were determined using a DMA SDTA861e (Mettler-Toledo Instruments). The samples in thickness of 1 mm were cut from those sheet samples prepared by compression molding. The testing was performed in three-point bending mode from 20 to 120 °C at a heating rate of 2 °C/min in N_2 atmosphere.

The crystallite morphology of PLA and PLAS film samples under the compressed CO_2 and after thermal annealing were studied using a polarized optical microscope (POM, Olympus BX 51TF) equipped with a camera DP71.

RESULTS AND DISCUSSION

In this study, the spherical nanosilica was compounded with PLA via melt processing. The nanosilica dispersion on the PLA matrix before foaming was characterized first. Then the effect of the nanosilica particle on the cell morphology of PLAS foams was investigated based on the formed crystallite size of PLA during the CO_2 saturation process.

dx.doi.org/10.1021/ie302281c | Ind. Eng. Chem. Res. 2013, 52, 6390−6398

Nanosilica Dispersion in PLA Matrix. Figure 1 shows SEM images of the resultant PLAS nanocomposites with

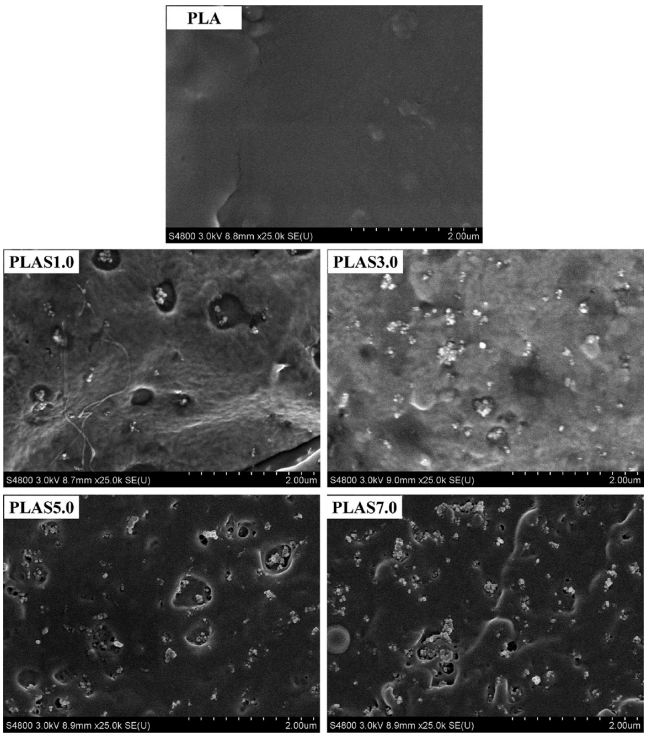

Figure 1. SEM micrographs of the fractured surfaces of PLAS samples.

different silica contents. It is seen clearly that PLAS7.0 has plentiful well-scattered multisilica aggregates after melt compounding. With decreasing the nanosilica content from the mater batch, the number of aggregates reduced, while the size and dispersion of aggregates did not change obviously. It indicates that the aggregates in the mater batch were not redispersed or further aggregated by the dilution processing in the mixer. Although the melt-processing was ineffective to disperse the nanosilica particles individually in PLA, the hydrophilic character of the nanosilica improved the interaction with PLA[21] and reduced the aggregate's degree of nanosilica in PLA.

The TEM micrograph was used to show the actual size of aggregates in PLA with two different nanosilica contents. As indicated in Figure 2, the irregular-shaped nanosilica aggregates with size of about 100−200 nm were dispersed uniformly on PLAS1.0 and PLAS3.0 samples. The TEM with high magnifications indicated that the size of single nanosilica particle was about 10 nm and each aggregate included more than 10 nanosilica particles. It was believed that the poor shear ability of the mini-lab compounder resulted in the formation of the large-sized nanosilica aggregates.

Influence of Nanosilica Addition on the Foaming Behaviors of PLA. Figure 3 shows the influence of nanosilica addition on the cell morphology of PLA foams, where the samples were saturated at 5 MPa and foamed at 70 °C for 20 s. As expected, PLA foam presented poor cell structure and showed obvious unfoamed regions.[7] Different from PLA foam, PLAS0.5 and PLAS1.0 foams exhibited uniform cell distribution, elliptical cell structure, and a thin cell wall. At a high nanosilica content of 3.0 wt %, however, it is seen that the cell structures of PLAS3.0 foam were developed into the long

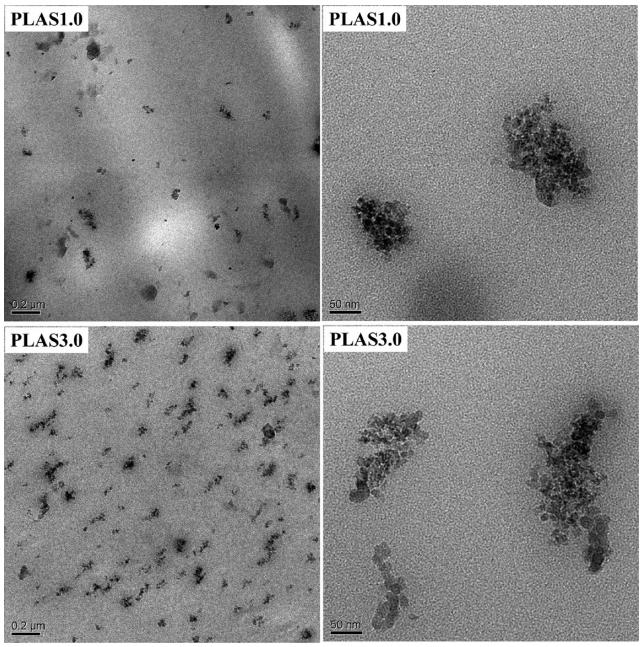

Figure 2. TEM micrographs of PLAS1.0 and PLAS3.0 with various magnifications.

elliptical shape and even to the triangle shape. At higher nanosilica contents of 5.0 and 7.0 wt %, the PLAS5.0 and PLAS7.0 foams kept a similar cell structure with PLAS3.0 foam, but the distribution of cell structure was somewhat nonuniform due to the presence of tiny cells in some regions as noted by the arrows.

Figure 4 summarizes the results of the cell structure of PLAS nanocomposites foams as a function of silica content, including average cell size and cell density. It is shown that the average cell size increased slightly from 36.2 μm of PLA foam to 41.3 μm of PLAS0.5 foam. At higher silica contents, however, the average cell size of PLAS foams tended to decrease gradually to 34.1 μm of PLAS1.0 foam, 23.9 μm of PLAS3.0 foam, 15.1 μm of PLAS5.0 foam, and 11.2 μm of PLAS7.0 foam. On the other hand, the cell density increased remarkably from 6.4×10^6 cells/cm^3 of PLA foam to 2.6×10^7 cells/cm^3 of PLAS0.5 foam, and then gradually increased with a further increase in the silica content. For PLAS7.0 foam, the cell density, 2.4×10^9 cells/cm^3, was almost 2 orders of magnitude higher than that of PLAS0.5 foam. Compared with the cell structure of PLA foam, those of PLAS foams were improved greatly with the addition of nanosilica up to 7 wt %.

The cell size is an important parameter by which to characterize the cell growth behavior of polymeric foaming, and the stiffness of the polymer matrix has been verified as a critical factor to determine the cell growth.[22] Table 1 summarizes the storage modulus of PLA and PLAS nanocomposites at 40 °C measured by DMA. It is seen that PLA, PLAS0.5, and PLAS1.0 possessed the similar storage modulus of 1944.5−1959.7 MPa at their glass state. With the increase in nanosilica content, however, the storage modulus of PLAS samples significantly increased up to 2468.7 MPa of PLAS3.0, 2831.2 MPa of PLAS5.0, and 2918.5 MPa of PLAS7.0, respectively. The high matrix stiffness restricted the cell growth, which combined with the enhanced heterogeneous nucleation,[23] led to the obvious decrease in cell size of PLAS foams at high nanosilica content.

dx.doi.org/10.1021/ie302281c | Ind. Eng. Chem. Res. 2013, 52, 6390−6398

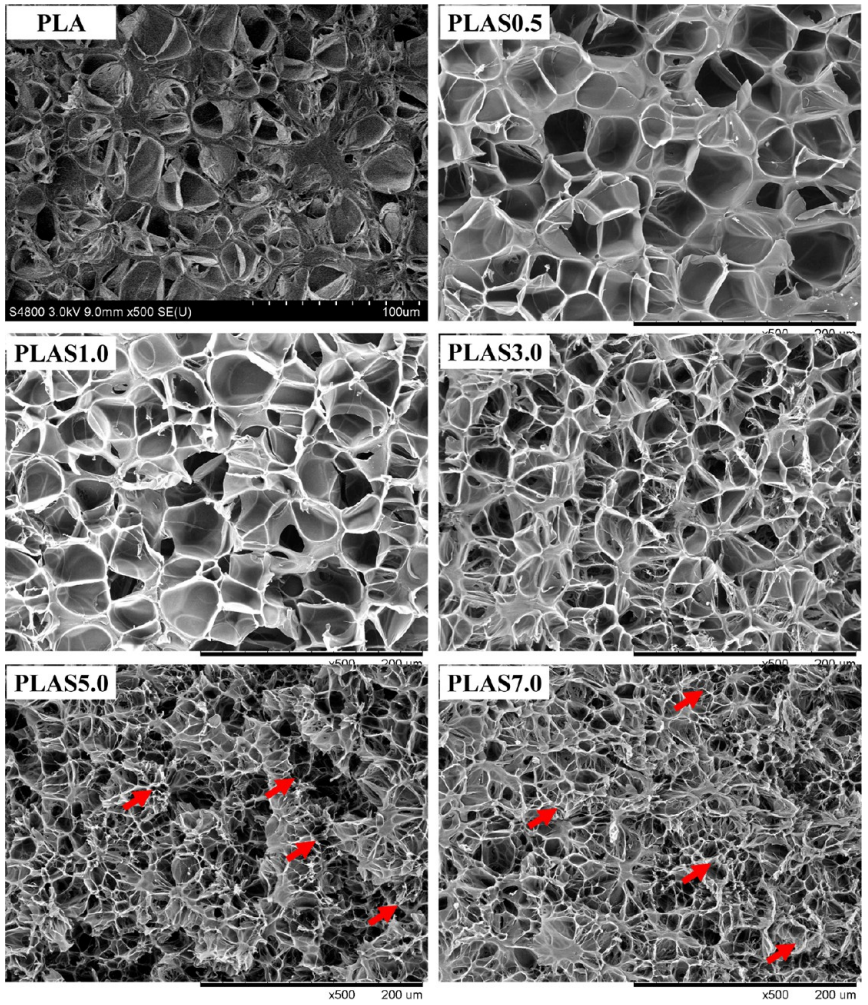

Figure 3. Cell morphologies of PLAS foams saturated at 5 MPa and foamed at 70 °C for 20 s.

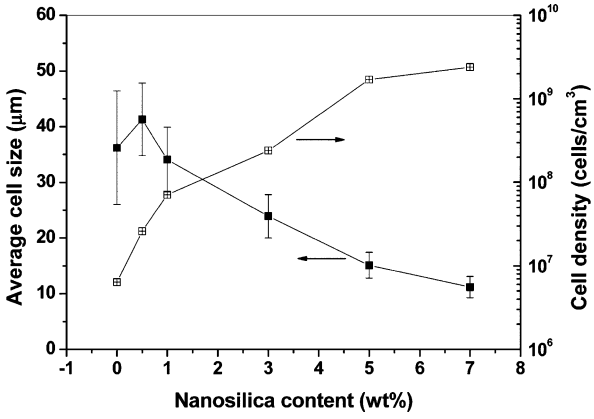

Figure 4. Average cell size and cell density of PLA and PLAS nanocomposites foams saturated at 5 MPa and foamed at 70 °C for 20 s.

Figure 5 shows the influence of foaming temperature on the cell morphology of PLAS0.5 and PLAS5.0 foams. For PLAS0.5, it could foam at 60 °C and the resultant foam exhibited an elliptical cell structure and uniform cell distribution. Furthermore, the increase in foaming temperature tended to increase the cell size of PLAS0.5 foams gradually owe to the increased cell growth rate at high foaming temperature.[24] For PLAS5.0, however, the resultant foam at 60 °C possessed nonuniform cell distributions, small cell sizes, and the unfoamed regions, resulting from the restricted cell growth because of high matrix stiffness of PLAS at high nanosilica loading. The increase in foaming temperature facilitated the elimination of the unfoamed regions but did not affect the cell size of PLAS5.0 foams obviously.

The expansion ratio is a critical data to present the foaming behavior of polymers, and a high expansion ratio can effectively reduce the resin usage. Figure 6 shows the influence of foaming temperature and nanosilica content on the expansion ratio of PLA foams. At the foaming temperature of 60−80 °C, it is seen that the increase in foaming temperature increased the expansion ratio of PLA foams from 1.7 to 9.6. The addition of nanosilica presented the obvious effect on the expansion ratio of PLA foams. The highest expansion ratio of 19.2, 15.7,

Table 1. Storage Modulus of PLA and PLAS Nanocomposites at 40 °C

samples	PLA	PLAS0.5	PLAS1.0	PLAS3.0	PLAS5.0	PLAS7.0
storage modulus (MPa)	1944.5	1951.5	1959.7	2468.7	2831.2	2918.5

dx.doi.org/10.1021/ie302281c | Ind. Eng. Chem. Res. 2013, 52, 6390−6398

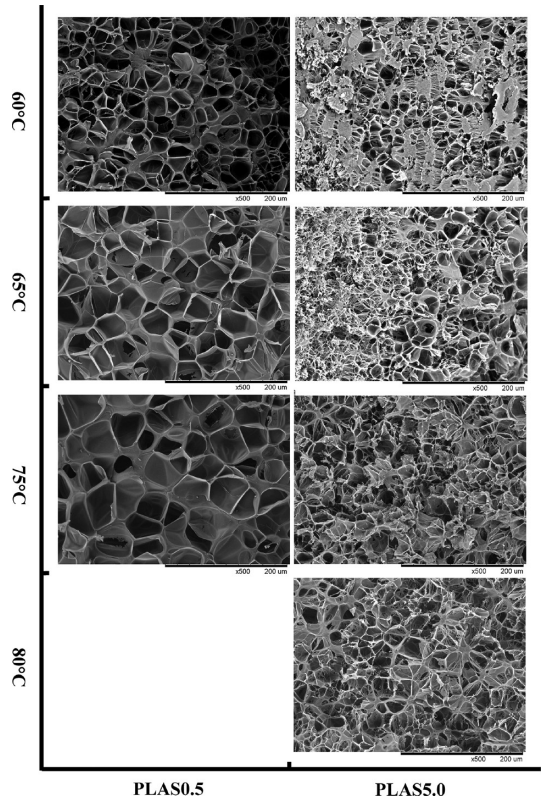

Figure 5. SEM micrographs of PLAS0.5 and PLAS5.0 nanocomposites foams obtained at various foaming temperatures.

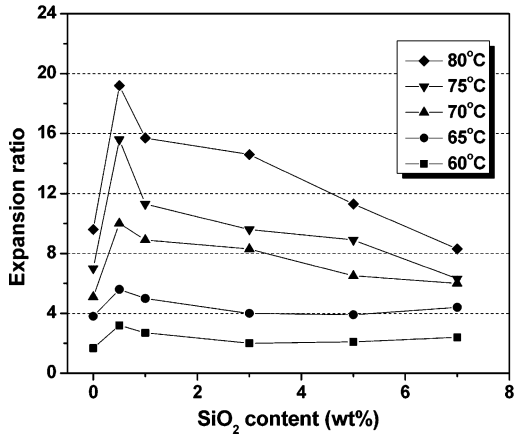

Figure 6. Expansion ratio of PLAS nanocomposites foams obtained at various foaming temperatures.

14.3, 11.3, and 8.3 was obtained at the highest foaming temperature of 80 °C for PLAS0.5, PLAS1.0, PLAS3.0, PLAS5.0, and PLAS7.0, respectively. An important feature of expansion ratio was the presence of mountain shape as a function of nanosilica content, and the 0.5 wt % was the optimum content. The improved cell nucleation and the favorable cell growth due to the low matrix stiffness at this condition were the possible reasons for this phenomenon.

Mechanisms of the Influence of Crystallite Size on the Foaming Behavior of PLAS. In the solid state foaming, the foaming behavior of PLA is significantly affected by the induced crystallinity of PLA after the CO_2 saturation.[7] As shown in Figure 7 and Table 2, the induced crystallinity of PLA at 5 MPa was 23.0%, and the addition of nanosilica tended to increase the

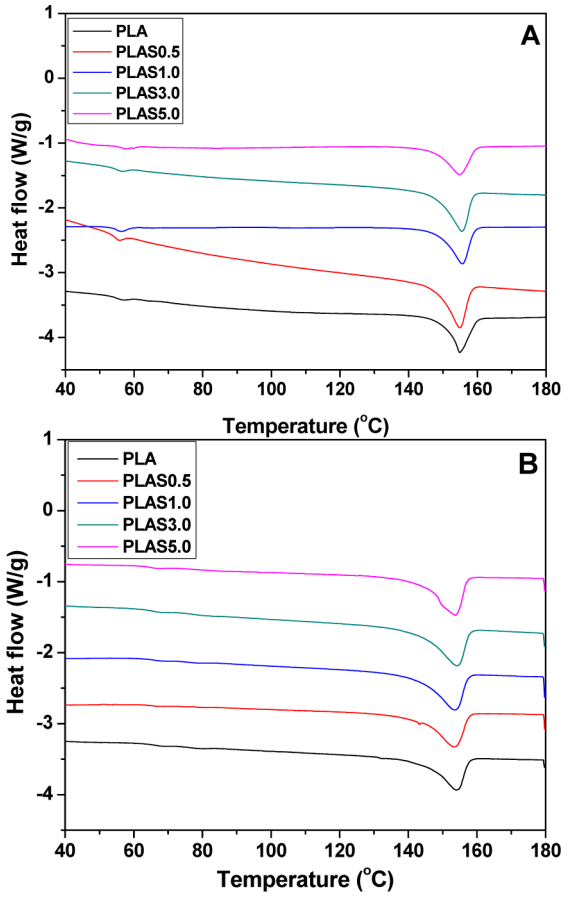

Figure 7. DSC thermographs of PLA and PLAS after CO_2 saturation (A) and microcellular foaming (B).

induced crystallinity of PLA obviously, i.e., 29.7% of PLAS0.5, 29.1% of PLAS1.0, 28.4% of PLAS3.0, 27.8% of PLAS5.0, and 27.2% of PLAS7.0. In addition, the crystallinity of PLA foam was 28.2%, and the introduction of nanosilica significantly increased the crystallinities of PLAS nanocomposites foams up to 36.5%. As indicated in Figure 2, the cell morphology of the resultant PLA foam was nonuniform. The possible reason was that the nucleation in the multiple-phase system was nonuniform. Near the solid filler such as the crystalline domain,[25,26] the growth of the nucleated bubbles generated the local strain field variation,[27,28] which enhanced the crystallization process.[9] The resultant high crystallinity suppressed cell growth and thereby induced a nonuniform cell structure in the foams.[7] On the basis of this hypothesis, PLAS nanocomposites with higher induced crystallinity were expected to exhibit much poorer cell structure. On the contrary, as indicated in Figures 3 and 5, PLAS nanocomposites foams possessed the obvious improved cell morphology compared to that of PLA foam. This suggested that besides the crystallinity, other crystallite properties such as crystallite size and crystallite density might play a key role in determining the foaming behavior of the semicrystalline PLA.

In the previous study,[6] on the basis of the SEM observation, we had observed the actual crystallite structure with the size of 30−40 μm in the junction of cells within the PLA foams. In addition, it was found that the cell structure of the PLA foam was nonuniform once the spherulite crystallite was present. In this study, however, the PLAS foams exhibited a uniform cell structure and thin wall with a size of 3−5 μm, as indicated in Figure 2. This phenomenon suggested that the size of the

dx.doi.org/10.1021/ie302281c | Ind. Eng. Chem. Res. 2013, 52, 6390−6398

Table 2. Crystallinity of PLA and PLAS Nanocomposites Saturated at 5 MPa and 20 °C and Foamed at 70 °C for 20 s

samples		PLA	PLAS0.5	PLAS1.0	PLAS3.0	PLAS5.0	PLAS7.0
crystallinity	saturated	23.0%	29.7%	29.1%	28.4%	27.8%	27.2%
	foamed	28.2%	33.6%	35.8%	36.5%	35.1%	36.1%

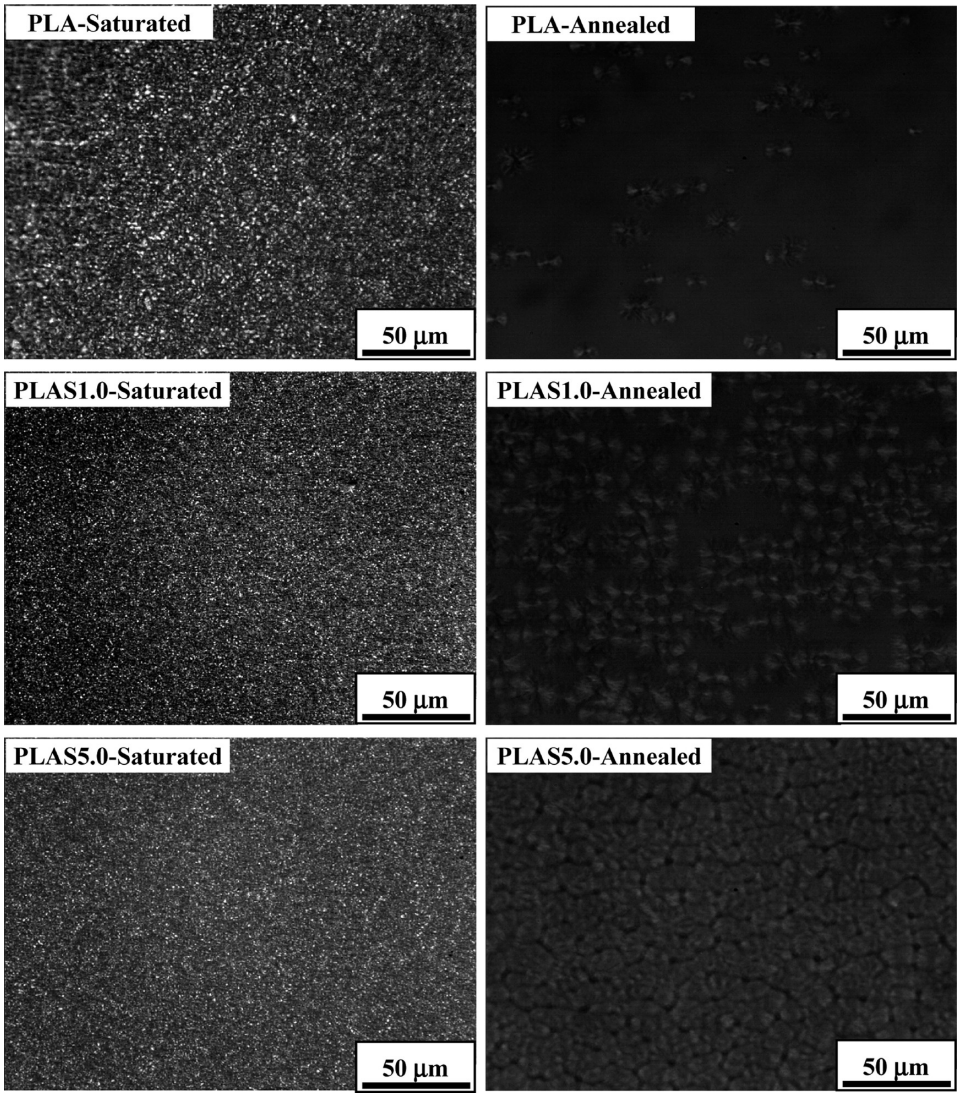

Figure 8. POM of PLA and PLAS nanocomposites saturated at 5 MPa and 20 °C for 12 h and annealed at 85 °C for 2 h.

crystal domain formed during the foaming should be less than 3−5 μm.

Figure 8 shows the crystallite morphology of PLA and PLAS nanocomposites saturated at 5 MPa and 20 °C for 12 h and annealed at 85 °C for 2 h, where the samples possessed similar crystallinity at the two conditions as indicated in Table 3 and Figure 9. It is seen that the saturated PLA and PLAS samples exhibited much smaller crystallite size and much higher crystallite density than the annealed samples. In addition, the introduction of nanosilica was observed to reduce the crystallite

Table 3. Crystallinity of PLAS Nanocomposites Saturated at 5 MPa and 20 °C for 12 h and Annealed at 85 °C for 2 h

samples		PLA	PLAS1.0	PLAS5.0
crystallinity	saturated	23.0%	28.1%	27.8%
	annealed	24.1%	29.7%	28.2%

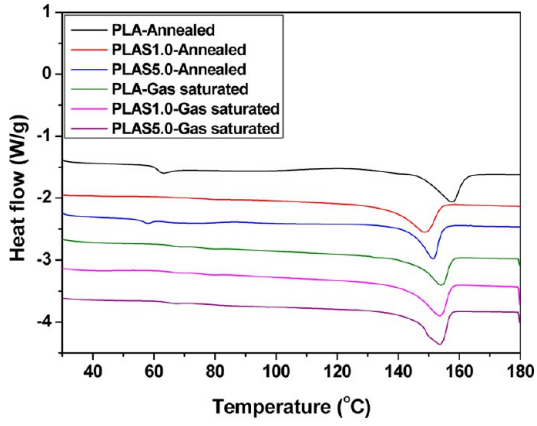

Figure 9. DSC thermographs of PLA and PLAS after annealed at 85 °C for 2 h and CO_2 saturation at 5 MPa and 20 °C for 12 h.

dx.doi.org/10.1021/ie302281c | Ind. Eng. Chem. Res. 2013, 52, 6390−6398

size of PLA, and an increase in the nanosilica content tended to decrease the crystallite size of PLA gradually. A similar phenomenon had been observed by researchers using the light scattering technique,[5] and it was clarified that the spherulite size decreased with decreasing CO_2 treatment temperature and the morphological transition from spherulites on a micrometer scale to rodlike crystalline superstructures on a nanometer scale occurs around 15 °C under 7−15 MPa and around 30 °C under 3 MPa. On the other hand, the crystallite structure of PLA annealed at 80−90 °C in air was microspherulites.

The isothermal crystallization kinetics of PLA and PLAS under atmospheric pressure was measured with the aim to show the influence of nanosilica addition on the crystal nucleation and growth kinetics. The authoritative Avrami equation was used to describe the isothermal crystallization.

$$X(t) = 1 - \exp(-kt^n) \quad (3)$$

$$\log[-\ln(1 - X(t))] = n \log t + \log k \quad (4)$$

where $X(t)$ is relative crystallinity at crystallization time, n is the Avrami exponent, and k is the crystallization rate constant. The plot of relative crystallinity is shown in Figure 10A, and the

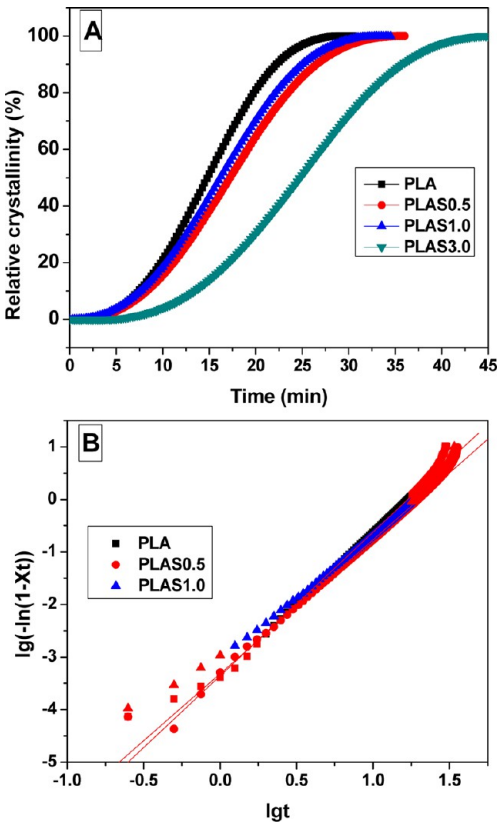

Figure 10. Curves of relative crystallinity vs crystallization time (a) and the Avrami plots of melt crystallization (b) for PLA and PLAS samples.

obtained values of crystallization half-time ($t_{1/2}$) are listed in Table 4. It is clear that the values of $t_{1/2}$ increased with the presence of nanosilica, which illustrated that the nanosilica decreased the crystallization rate of PLA. Avrami plots are shown in Figure 10B, and the values of Avrami exponent are obtained and listed in Table 4. PLA had the n value of 2.73, and

Table 4. Kinetic Parameters from the Avrami Analysis for PLA and PLAS Samples

samples	n	$t_{1/2}$
PLA	2.73	14.7
PLAS0.5	2.54	17.3
PLAS1.0	2.50	16.3

the introduction of nanosilica decreased the n values to 2.54 of PLAS0.5 and to 2.50 of PLAS1.0. This confirmed that the nanosilica acted as a heterogeneous nucleating agent to enhance the crystal nucleation.

Using the cell nucleation mechanism newly proposed by Leung et al.,[27] Wong et al.,[28,29] and Wang et al.,[30] we previously explained the mechanism of the formation of the unfoamed regions and nonuniform cell size distribution in PLA foam based on the local stress variation.[7] As mentioned above, the introduction of nanosilica significantly decreased the crystallite size of PLA under the compressed CO_2. Both the well dispersed tiny crystal domains and nanosilica aggregates induced the uniform cell nucleation, which decreased the number of the prenucleated bubbles and thereby reduced the intensity of the generated local strain field variation. As a result, this weakened the potential crystallite development in those areas. Furthermore, the introduction of nanosilica decreased the crystal growth rate, which reduced the increase in polymer matrix stiffness and thereby facilitated the cell growth process. We believed that both the improved cell nucleation and cell growth endowed PLAS foams with the well-defined cell morphology and the increased expansion ratio, even though they possessed high induced crystallinity after CO_2 saturation. The formation of tiny crystallite size in the saturated PLAS samples was thought to be the key reason for this interesting phenomenon.

Influence of Foaming Process on the Dispersion of Nanosilica. Figure 11 shows the SEM micrographs of PLAS3.0 and PLA5.0 foams with different magnifications, where the foams were obtained at the foaming temperature of 75 °C. For PLAS3.0 foam, at a low magnification of ×6000, a larger amount of white nanosilica particles were observed in the cell wall and the junction of three contacting cells. At a high magnification of ×20 000, the well dispersed nanosilica particles sized at about 20−30 nm were found on the cell wall. For the junction of three contacting cells, however, the nanosilica aggregates possessed a much large size, i.e., 50−100 nm, and nonuniform distribution. It is interesting to note that PLAS5.0 foam with high nanosilica loading exhibited a much larger nanosilica aggregate size of about 50−500 nm at the cell junction and of about 20−80 nm on the cell wall. As mentioned in Figure 1, the nanosilica content did not present an obvious effect on the shape and size of the nanosilica aggregates. This suggested that the foaming process might further affect the dispersion of nanosilica in the PLA matrix.

It is known that the nanoparticles-induced heterogeneous cell nucleation has a lower energy barrier than homogeneous nucleation, and it preferentially occurs on the rough surfaces of nanoparticles.[31] The used nanosilica particles in this study possesses a high specific surface area, and the irregular-shaped nanosilica aggregates in the PLA matrix inevitably contain conical pits due to surface roughness. The trapped gas might develop into the prenucleated nuclei and then induce the occurrence of cell nucleation around nanosilica aggregates during the foaming.[31] The followed gas diffusion promoted the

dx.doi.org/10.1021/ie302281c | Ind. Eng. Chem. Res. 2013, 52, 6390−6398

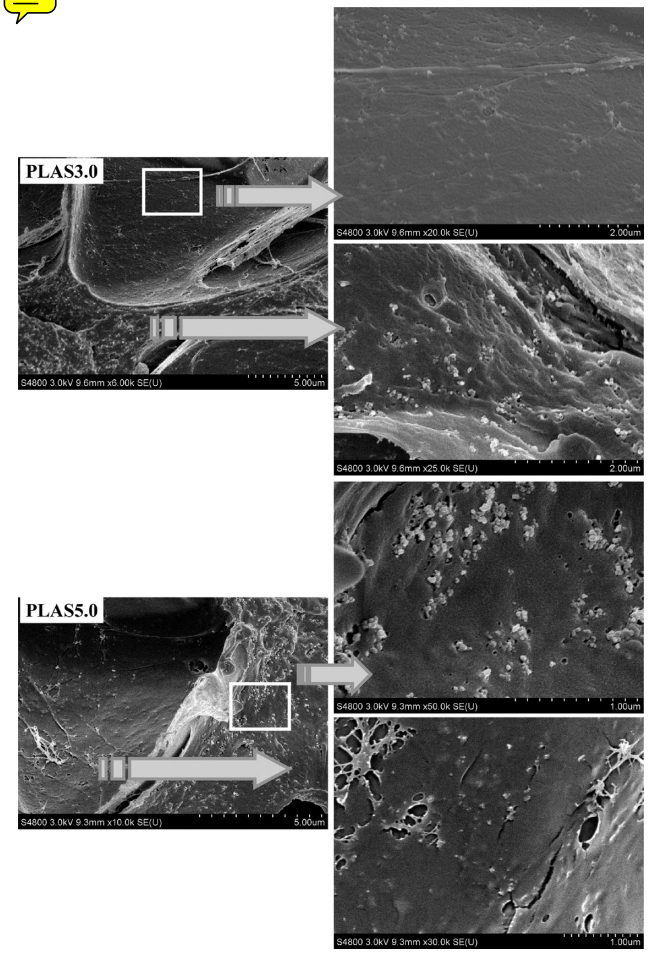

Figure 11. SEM micrographs illustrating the effect of the foaming process on the dispersion of nanosilica.

bubble growth, which generated a strong extensional action onto the cell wall. Given the interface bonding between the polymer matrix and the nanoparticles, the applied biaxial stretching action during cell growth was expected to transfer from the matrix onto the nanoparticles. This process tended to redisperse the nanoparticles in the foamed samples.[32,33] Okamoto et al.'s previous study suggested that different regions possessed different values of extensional flow during the foaming process, where the regions on the cell wall was strong extensional flow while the junction regions of three contacting cells was stagnation flow.[34] Our previous simulation results also indicated that the generated extensional flow on the cell wall was as high as 82.7−179.4 s^{-1} during the cell growth process.[35] The formed strong stretching action facilitated the redispersion of nanosilica on the cell wall. At the junction regions of three contacting cells, however, the formed stagnation flow did not improve the dispersion of nanosilica aggregates. As mentioned above, PLAS nanocomposites foams exhibited different expansion behavior as the function of nanosilica content. PLAS samples with high nanosilica contents possessed high matrix stiffness and thereby restricted cell growth and foam expansion. The reduced stretching action reduced the redispersion ability of nanosilica aggregates in PLAS5.0 foam during expansion.

CONCLUSIONS

In this study, the microcellular foaming behavior of PLA and PLAS samples was investigated by using the compressed CO_2 as the physical blowing agent. The prepared PLA foams at 5 MPa had unfoamed regions and a low expansion ratio. On the basis of the newly proposed cell nucleation mechanism, this phenomenon was attributed to the nonuniform cell nucleation due to the presence of crystal domains and the suppressed cell growth due to the enhanced crystallization development in some local areas. The introduction of nanosilica was verified to significantly improve the foaming behavior of PLA, even though the saturated PLAS samples possessed higher induced crystallinities than the saturated PLA. A further crystal morphology observation and crystallization kinetics analysis indicated that the presence of nanosilica decreased the crystallite size and crystal growth rate of PLA. The well dispersed crystal domains and nanosilica aggregates with small sizes induced the occurrence of uniform cell nucleation. This phenomenon accompanying with the decreased crystallization development of PLA matrix during the cell growth process facilitated the foam expansion of PLAS samples. The foaming process was found to redisperse the nanosilica aggregates in PLA foams. The cell wall regions had a much smaller aggregates size than the cell junction regions, i.e., 20−30 nm vs 50−100 nm in PLAS3.0 foam and 50−100 nm vs 50−500 nm in PLAS5.0 foam, which was attributed to the formation of a stronger extension action on the cell wall during foaming.

AUTHOR INFORMATION

Corresponding Author

*E-mail: wtzhai@nimte.ac.cn (W.Z.); jdwcheju@jejunu.ac.kr (D.W.J.).

Notes

The authors declare no competing financial interest.

ACKNOWLEDGMENTS

We gratefully acknowledge the financial support of the National Natural Science Foundation of China (Grant 51003115).

REFERENCES

(1) Gupta, B.; Revagade, N.; Hilborn, J. Poly(lactic acid) Fiber: An Overview. *Prog. Polym. Sci.* **2007**, *32*, 455−482.
(2) Södegård, A.; Stolt, M. Properties of Lactic Acid Based Polymers and Their Correlation with Composition. *Prog. Polym. Sci.* **2002**, *27*, 1123−1163.
(3) Auras, R.; Harte, B.; Selke, S. An Overview of Polylactides as Packaging Materials. *Macromol. Biosci.* **2004**, *4*, 835−864.
(4) Lim, L. T.; Auras, R.; Rubino, M. Processing Technologies for Poly(lactic acid). *Prog. Polym. Sci.* **2008**, *33*, 820−852.
(5) Marubayashi, H.; Akaishi, S.; Akasaka, S.; Asai, S.; Sumita, M. Crystalline Structure and Morphology of Poly(L-Lactide) Formed under High-Pressure CO_2. *Macromolecules* **2008**, *41*, 9192−9203.
(6) Zhai, W. T.; Ko, Y.; Zhu, W. L.; Wong, A.; Park, C. B. A Study of the Crystallization, Melting, and Foaming Behaviors of Polylactic Acid in Compressed CO_2. *Int. J. Mol. Sci.* **2009**, *10*, 5381−5397.
(7) Wang, J.; Zhai, W. T.; Ling, J. Q.; Shen, B.; Zheng, W. G.; Park, C. B. Ultrasonic Irradiation Enhanced Cell Nucleation in Microcellular Poly(lactic Acid): A Novel Approach to Reduce Cell Size Distribution and Increase Foam Expansion. *Ind. Eng. Chem. Res.* **2011**, *50*, 13840−13847.
(8) Mihai, M.; Huneault, M. A.; Favis, B. D. Crystallinity Development in Cellular Poly(lactic acid) in the Presence of Supercritical Carbon Dioxide. *J. Appl. Polym. Sci.* **2009**, *113*, 2920−2932.

(9) Wang, J.; Zhu, W.; Zhang, H.; Park, C. B. Continuous Processing of Low-Density, Microcellular Poly(lactic acid) Foams with Controlled Cell Morphology and Crystallinity. *Chem. Eng. Sci.* **2012**, *75*, 390−399.
(10) Wang, X. X.; Kumar, V.; Li, W. Low Density Sub-Critical CO_2-Blown Solid-State PLA Foams. *Cell. Polym.* **2007**, *26*, 11−35.
(11) Lan, Q. F.; Yu, J.; He, J. S.; Maurer, F. H. J.; Zhang, J. Thermal Behavior of Poly(L-lactide) Having Low L-Isomer Content of 94% after Compressed CO_2 Treatment. *Macromolecules* **2010**, *43*, 8602−8609.
(12) Liao, X.; Nawaby, A. V.; Whitfield, P.; Day, M.; Champagne, M.; Denault, J. Layered Open Pore Poly(L-lactic acid) Nanomorphology. *Biomacromolecules* **2006**, *7*, 2937−2941.
(13) Doroudiani, S.; Park, C. B.; Kortschot, M. T. Processing and Characterization of Microcellular Foamed High-Density Polyethylene/Isotactic Polypropylene Blends. *Polym. Eng. Sci.* **1998**, *38*, 1205−1215.
(14) Mizumoto, T.; Sugimura, N.; Moritani, M.; Sato, Y.; Masuoka, H. CO_2-Induced Stereocomplex Formation of Stereoregular Poly(methyl methacrylate) and Microcellular Foams. *Macromolecules* **2000**, *33*, 6757−6763.
(15) Lips, P. A. M.; Velthoen, I. W.; Dijkstra, P. J.; Wessling, M.; Feijen, J. Gas Foaming of Segmented Poly(ester amide) Films. *Polymer* **2005**, *46*, 9396−9403.
(16) Ema, Y.; Ikeya, M.; Okamoto, M. Foam Processing and Cellular Structure of Polylactide-Based Nanocomposites. *Polymer* **2006**, *47*, 5350−5359.
(17) Mascia, L.; Del Re, G.; Ponti, P. P.; Bologna, S.; Di Giacomo, G.; Haworth, B. Crystallization Effects on Autoclave Foaming of Polycarbonate Using Supercritical Carbon Dioxide. *Adv. Polym. Tech.* **2006**, *25*, 225−235.
(18) Zhai, W. T.; Wang, H. Y.; Yu, J.; Dong, J. Y.; He, J. S. Foaming Behavior of Isotactic Polypropylene in Supercritical CO_2 Influenced by Phase Morphology via Chain Grafting. *Polymer* **2008**, *49*, 3146−3156.
(19) Zhai, W. T.; Kuboki, T.; Wang, L. L.; Park, C. B.; Lee, E. K.; Naguib, H. E. Cell Structure Evolution and the Crystallization Behavior of Polypropylene/Clay Nanocomposites Foams Blown in Continuous Extrusion. *Ind. Eng. Chem. Res.* **2010**, *49*, 9834−9845.
(20) Fischer, E. W.; Sterzel, H. J.; Wegner, G. Investigation of the Structure of Solution Grown Crystals of Lactide Copolymers by Means of Chemical Reaction. *Kolloid-Z. Z.-Polym.* **1973**, *251*, 980−990.
(21) Dorigato, A.; Sebastiani, M.; Pegoretti, A.; Fambri, L. Effect of Silica Nanoparticles on the Mechanical Performances of Poly(lactic acid). *J. Polym. Environ.* **2012**, *20*, 713−725.
(22) Wang, J.; Cheng, X. G.; Yuan, M. J.; He, J. S. An Investigation on the Microcellular Structure of Polystyrene/LCP Blends Prepared by using Supercritical Carbon Dioxide. *Polymer* **2001**, *42*, 8265−8275.
(23) Zhai, W. T.; Yu, J.; Wu, L. C.; Ma, W. M.; He, J. S. Heterogeneous Nucleation Uniformizing Cell Size Distribution in Microcellular Nanocomposites Foams. *Polymer* **2006**, *47*, 7580−7589.
(24) Arora, K. A.; Lesser, A. J.; McCarthy, T. J. Preparation and Characterization of Microcellular Polystyrene Foams Processed in Supercritical Carbon Dioxide. *Macromolecules* **1998**, *31*, 4614−4620.
(25) Baldwin, D. F.; Park, C. B.; Suh, N. P. A Microcellular Processing Study of Poly(ethylene terephthalate) in the Amorphous and Semicrystalline Sstates. 1. Microcell Nucleation. *Polym. Eng. Sci.* **1996**, *36*, 1437−1445.
(26) Baldwin, D. F.; Park, C. B.; Suh, N. P. A Microcellular Processing Study of Poly(ethylene terephthalate) in the Amorphous and Semicrystalline States. 2. Cell Growth and Process Design. *Polym. Eng. Sci.* **1996**, *36*, 1446−1453.
(27) Leung, S. N.; Wong, A.; Wang, C.; Park, C. B. Mechanism of Extensional Stress-Iinduced Cell Formation in Polymeric Foaming Processes with the Presence of Nucleating Agents. *J. Supercrit. Fluids* **2012**, *63*, 187−198.
(28) Wong, A.; Park, C. B. The Effects of Extensional Stresses on the Foamability of Polystyrene-Talc Composites Blown with Carbon Dioxide. *Chem. Eng. Sci.* **2012**, *75*, 49−62.
(29) Wong, A.; Park, C. B. A Visualization System for Observing Plastic Foaming Processes Under Shear Stress. *Polym. Test.* **2012**, *31*, 417−424.
(30) Wang, C.; Leung, S. N.; Bussmann, M.; Zhai, W. T.; Park, C. B. Numerical Investigation of Nucleating Agent-Enhanced Heterogeneous Nucleation. *Ind. Eng. Chem. Res.* **2010**, *49*, 12783−12792.
(31) Leung, S. N.; Park, C. B.; Li, H. B. Effects of Nucleating Agents' Shapes and Interfacial Properties on Cell Nucleation. *J. Cell. Plast.* **2010**, *46*, 441−460.
(32) Zhai, W. T.; Park, C. B.; Kontopoulou, M. Nanosilica Addition Dramatically Improves the Cell Morphology and Expansion Ratio of Polypropylene Heterophasic Copolymer Foams Blown in Continuous Extrusion. *Ind. Eng. Chem. Res.* **2011**, *50*, 7782−7289.
(33) Zheng, W. G.; Lee, Y. H.; Park, C. B. Use of Nanoparticles for Improving the Foaming Behaviors of Linear PP. *J. Appl. Polym. Sci.* **2010**, *117*, 2972−2979.
(34) Okamoto, M.; Nam, P. H.; Maiti, P.; Kotaka, T.; Nakayama, T.; Takada, M.; Ohshima, M.; Usuki, A.; Hasegawa, N.; Okamoto, H. Biaxial Flow-Induced Alignment of Silicate Layers in Polypropylene/Clay Nanocomposite Foam. *Nano Lett.* **2001**, *1*, 503−505.
(35) Zhai, W. T.; Wang, J.; Chen, N.; Naguib, H. E.; Park, C. B. The Orientation of Carbon Nanotubes in Poly(ethylene-co-octene) Microcellular Foaming. *Polym. Eng. Sci.* **2012**, *52*, 2078−2089.